Clays and Clay Minerals, Vol. 41, No. 4, 472–483, 1993.

PROPERTIES AND CHARACTERIZATION OF Al_2O_3 AND SiO_2-TiO_2 PILLARED SAPONITE

P. B. MALLA[1] AND S. KOMARNENI*[2]

[1] Research and Development, Thiele Kaolin Company, P.O. Box 1056
Sandersville, Georgia 31082

[2] Materials Research Laboratory, The Pennsylvania State University
University Park, Pennsylvania 16802

Abstract—A saponite pillared with a single (Al_2O_3) or a mixed (SiO_2-TiO_2) oxide exhibited basal spacings of 16–19 and 30–40 Å, respectively. The pillared structures were found to be stable up to 700°C. Water, nitrogen, and high resolution argon adsorption were used to study the effect of thermal treatments on surface chemistry, pore structure, and surface area of these pillared clays. The pillared saponites exhibited a hydrophobic behavior at temperatures >500°C, whereas such behavior was observed at ≥300°C for montmorillonite. Most of the micropores in the Al_2O_3 pillared clays were <10 Å, whereas the SiO_2-TiO_2 pillared clays showed a broad distribution of pores in both micropore and mesopore regions. The SiO_2-TiO_2 pillared samples possessed higher surface area compared with Al_2O_3 pillared clays. The percent decrease in surface area was smaller for pillared saponites compared with pillared montmorillonites when calcined from 300° to 700°C, indicating a higher thermal stability of the former. The pillared clays were also characterized by solid state ^{27}Al and ^{29}Si magic-angle spinning nuclear magnetic resonance (MAS/NMR) spectroscopy. There was no direct evidence of cross-linking (covalent bonding between the clay layer and pillar) in montmorillonite irrespective of the types of pillars. In saponite, however, a significant structural modification took place. ^{27}Al spectra of Al_2O_3 pillared saponite heated at ≥300°C appear to indicate an increase in Al^{VI} as a result, at least in part, of initiation of hydrolytic splitting of Si-O-Al bonds. The actual release of Al from the tetrahedral sheet probably occurred at a temperature >500°C and completed around 700°C with the formation of Si-O-Si linkages. The decreased intensity of peak due to Si(1Al) in ^{29}Si spectra of the sample heated at 700°C corroborates the ^{27}Al MAS/NMR results. Additionally, the ^{29}Si spectra indicated a cross-linking between SiO_4 (clay sheet) with Al_2O_3 pillars, which could be achieved by inverting some silica tetrahedra into the interlayer. ^{27}Al and ^{29}Si spectra of SiO_2-TiO_2 pillared saponite also showed the trend similar to that exhibited by Al_2O_3 pillared saponite, indicating that the crystal chemistry of the host may be more important than the nature of pillars in the structural modification and cross-linking behavior of thermally treated pillared clays.

Key Words—Adsorption, Clays, Cross-linking, MASNMR, Montmorillonite, Pillared clay, Saponite, Smectite.

INTRODUCTION

Smectite clays show considerable swelling and can accommodate a variety of ions, metal clusters, and organic molecules in the interlayers as a result of their low layer charge (≤0.6/half unit cell). Various crystal chemical parameters such as magnitude of charge, site and distribution of layer charge, and nature of octahedral sheet (di- or trioctahedral) have been shown to influence various chemical and physical reactions occurring on the clay surfaces. Among these parameters, the effect of charge site (tetrahedral or octahedral) on various properties has been extensively studied, e.g., K fixation (Weir and White, 1951; van Olphen, 1966; Robert, 1973), swelling in glycerol (Harward and Brindley, 1965; Harward *et al.*, 1969; Malla and Douglas, 1987), bonding of water molecules (Cariati *et al.*, 1983), or surface acidity (Mortland and Raman, 1968). Cationic (isomorphous) substitution in the tetrahedral (e.g., beidellite, nontronite, saponite) sheet exerts a greater influence on the reactions above than those located in the octahedral sheet (e.g., montmorillonite, hectorite). This is due to the differences in ionic attraction for tetrahedral or octahedral charge sites as imposed by their distance from the interlayer positions.

Since the report of the first pillaring of organic molecules (tetraalkylammonium ion) in smectite by Barrer and MacLoed (1955), a variety of inorganic oxides, Al_2O_3 (Brindley and Sempels, 1977), ZrO_2 (Yamanaka and Brindley, 1979), TiO_2 (Yamanaka *et al.*, 1987; Sterte, 1986), Cr_2O_3 (Pinnavaia, 1985a), Ga_2O_3 (Bellaloui *et al.*, 1990), Al_2O_3-Ga_2O_3 (Gonzalez *et al.*, 1992), SiO_2-TiO_2 (Yamanaka *et al.*, 1988), and Al_2O_3-SiO_2 (Occelli, 1987; Sterte and Shabtai, 1987) have been successfully pillared in smectites to generate high surface area solids. These solids are potentially useful as catalysts, catalyst supports, molecular sieves, adsorbents, and sensors.

The small variation in the crystal chemistry of smectites influences both the structure and the properties of pillared clays. Plee *et al.* (1987) observed more ordered pillars in beidellite than in montmorillonite. The

* Also with the Department of Agronomy.

Table 1. Chemical analyses of Na- and pillared saponites and montmorillonites.

Oxide (%)[1]	NaM	APM	STPM	NaS	APS	STPS
SiO_2	64.86	60.03	74.28	58.44	53.46	68.23
Al_2O_3	24.14	33.29	11.45	5.04	14.63	2.93
TiO_2	0.15	0.14	12.05	0.03	0.06	10.71
Fe_2O_3	2.29	2.26	1.19	1.90	2.16	1.71
MgO	3.39	3.29	1.66	31.04	28.87	16.20
CaO	0.61	0.05	0.06	0.81	0.09	0.18
Na_2O	3.94	—	0.15	2.26	0.03	0.09
K_2O	0.10	—	—	0.03	—	—
Total	99.5	99.1	100.8	99.6	99.3	99.7

Structural formulas

NaM: $(K_{0.01}Na_{0.46}Ca_{0.04})(Mg_{0.30}Al_{1.57}Fe_{0.10})(Si_{3.87}Al_{0.13})O_{10}(OH)_2$

APM: $(Al_{0.83(p)}Ca_{0.04})(Mg_{0.32}Al_{1.57}Fe_{0.11})(Si_{3.87}Al_{0.13})O_{10}(OH)_2$

STPM: $(Si_{5.49}Ti_{1.2})_p(Mg_{0.31}Al_{1.57}Fe_{0.11})(Si_{3.87}Al_{0.13})O_{10}(OH)_2$

NaS: $(Na_{0.27}Ca_{0.05})(Mg_{2.87}Fe_{0.09})(Si_{3.63}Al_{0.37})O_{10}(OH)_2$

APS: $(Al_{0.80(p)}Ca_{0.01})(Mg_{2.92}Fe_{0.11})(Si_{3.63}Al_{0.37})O_{10}(OH)_2$

STPS: $(Na_{0.02}Ca_{0.02})(Si_{3.68}Ti_{0.86})_p(Mg_{2.59}Fe_{0.11})(Si_{3.63}Al_{0.37})O_{10}(OH)_2$

[1] Anhydrous basis (950°C); NaM, Na-montmorillonite; APM, Al_2O_3 pillared montmorillonite; STPM, SiO_2-TiO_2 pillared montmorillonite; NaS, Na-saponite; APS, Al_2O_3 pillared saponite; STPS, SiO_2-TiO_2 pillared saponite; p, pillar.

differences in the high-resolution NMR spectra of uncalcined and calcined pillared beidellite were interpreted as the consequence of inversion of some AlO_4 tetrahedra (tetrahedral sheet), which cross-link with the Al of the pillars (Plee *et al.*, 1985). The catalytic activities and selectivities of pillared beidellite were found to be higher than that of pillared montmorillonite due to the formation of Si-OH acid sites in the former (Schutz *et al.*, 1987). Besides catalytic activities, Malla *et al.* (1989) and Malla and Komarneni (1990a, 1990b) observed a definitive variation in water sorption isotherms for pillared montmorillonite, nontronite, hectorite, and saponite.

Although cross-linking was not observed in minerals having a negative charge in the octahedral sheet, Pinnavaia *et al.* (1985b) observed an inversion of Si tetrahedra and cross-linking between the Al in the pillars and the tetrahedral Si in calcined pillared fluorohectorite. This was attributed to the presence of F^- in the octahedral sheet of this material. Because of the high thermal stability of pillars, such cross-linking behavior was also assumed in hydroxy-Si/Al pillared fluorohectorite by Sterte and Shabtai (1987). Although cross-linking behavior in pillared montmorillonite, hectorite, beidellite, and nontronite have been studied, saponite has not been studied in detail. The objective of this study was, therefore, to characterize the adsorption and cross-linking properties of Al_2O_3 and SiO_2-TiO_2 pillared saponite. Relevant properties of pillared montmorillonite are presented for comparison.

MATERIALS AND METHODS

Host materials

Natural saponite and montmorillonite were used as host materials in this study. The saponite (SapCa-1) from Ballarat, California, was procured from the Source Clay Repository of the Clay Minerals Society. Less than 2.0 μm sized particles were separated by centrifugation (Jackson, 1969). The cation exchange capacity (CEC) was determined to be 79 meq/100 g. The Na-montmorillonite was supplied by Kunimine Industrial Co., Japan. The cation exchange capacity (CEC) was determined to be 113 meq/100 g. The chemical analyses and structural formulas of the raw materials and pillared clays are presented in Table 1.

Pillaring agents and pillaring process

Hydroxy-Al pillaring solution and pillaring process. A 0.4 M $AlCl_3 \cdot 6H_2O$ solution was titrated slowly with 0.4 M NaOH under constant and vigorous stirring using a magnetic stirrer. The OH/Al molar ratio of 2 was maintained. The resulting hydroxy-aluminum solution was aged at 60°C for 18 hr in a stoppered polypropylene bottle. An excess of pillaring solution (>30 times the CEC of the clay) was mixed with about 2–3 wt. % clay suspension and stirred at room temperature for 4 hr. A previous study has shown that a dilute clay-water slurry is not necessary for pillaring and that the pillaring solution may be directly added to dry clay (Malla and Komarneni, 1990a). After reaction, each product was washed four times with deionized water and filtered. The washed and filtered samples were then dried under a stream of dry air.

Silica-titania (SiO_2-TiO_2) pillaring solution-sol and pillaring. Silica-titania mixed sol was prepared following the method described by Yamanaka *et al.* (1988) with minor modification as described below. Typically for 1 g of clay (CEC = 1 meq), silica sol was prepared from 6.25 g tetraethylorthosilicate [$Si(OC_2H_5)_4$], 1.8 ml ethanol, and 1.5 ml 2 M HCl. The resulting solution was

stirred for 1 hr. For the same amount of clay, 0.85 g titanium (IV) isopropoxide [$Ti(OCH[CH_3]_2)_4$] was mixed with 3.4 g ethanol, resulting in a thick white slurry. No acid was added at this stage. The titania slurry was stirred for 5 min and then added to the above silica sol. The resulting mixture was stirred further for a period of 1 hr, giving rise to a yellowish, clear sol. The mixed sol thus prepared was mixed with 1% clay suspension and stirred at 50°C for 3 hr followed by washing five times with deionized water. The washed sample was dried at 60°C.

Chemical analysis

The samples were dissolved using the lithium metaborate fusion technique (Ingamells, 1970; Medlin *et al.,* 1969). K and Na were determined by flame emission spectrometry, while all other elements were determined by direct-current plasma emission spectroscopy (DCP).

X-ray powder diffraction analysis

A few drops of clay suspension were allowed to dry on glass slides at room temperature. Thermal stability of the pillared clays was studied after heating the slide mounts for at least 4 hr at 300°, 400°, 500°, 600°, and 700°C. XRD analyses of alumina pillared samples were performed with a Scintag diffractometer (4°/min) using Ni-filtered CuKα radiation. The SiO_2-TiO_2 pillared samples were analyzed by Philips APD 1700 diffractometer (2°/min) using graphite monochromated CuKα radiation.

Water and nitrogen adsorption

Water adsorption and desorption isotherms were measured by a volumetric method at 25°C using a computer-interfaced sorption apparatus (Yamanaka and Komarneni, 1991). Samples were degassed at 200°C after calcining at 400° for 20 hr or 700°C for 4 hr.

Nitrogen adsorption and desorption isotherms were measured using the Quantachrome Autosorb-1 at liquid N_2 temperature after degassing at 200°C. The samples were precalcined at 300°, 400°, and 500° for 20 hr and 700°C for 4 hr. Surface areas of Al_2O_3 pillared samples were estimated using both the BET and the Langmuir fit. With the BET equation, relative pressures <0.1 were used to achieve a positive slope. A relative pressure range of 0.05 to 0.30 was used with the Langmuir equation. Surface areas of SiO_2-TiO_2 pillared clays were also estimated from the BET fit in the relative pressure range of less than 0.1. Pore size distributions were calculated from adsorption isotherms using the BJH method (Barrett *et al.,* 1951). Micropore analysis of the SiO_2-TiO_2 pillared clays was performed at liquid Ar temperature using Ar as the probe molecule (ASAP 2000M, Micromeritics Instrument Corporation, One Micromeritics Drive, Norcross, Georgia). Micropore size distribution was calculated using the method developed by Horvath and Kawazoe (1983).

Magic-angle spinning nuclear magnetic resonance spectroscopy (MASNMR)

^{27}Al and ^{29}Si MASNMR spectra were recorded on either a Brucker (Model HX-360) or a ChemMagnetics (Model CMC 300A) instrument. The ^{27}Al chemical shift values were assigned relative to the 1M aqueous $AlCl_3$ reference solution, whereas the ^{29}Si chemical shift values were assigned with respect to the external standard tetramethylsilane (TMS).

RESULTS

Chemical analysis

Chemical analyses of the pillared and the original unpillared samples are presented in Table 1. The data illustrate the presence of higher amounts of Al_2O_3 or SiO_2 and TiO_2 in the pillared clays and show that almost all the original charge balancing cations (Na^+, Ca^{2+} or K^+) have been replaced by the pillaring species. The amount of the pillared species per $O_{20}(OH)_4$ unit can be estimated to be $1.66Al_p$, $10.98Si_p$, and $2.4Ti_p$ in montmorillonite and $1.60Al_p$, $7.38Si_p$, and $1.72Ti_p$ in saponite. The Si/Ti ratios of the pillared species were calculated to be 4.58 and 4.28 in montmorillonite and saponite, respectively, compared with the ratio of 10 for the original pillaring solution-sol.

X-ray powder diffraction analysis

XRD patterns of alumina and silica-titania pillared clays are presented in Figures 1 and 2. The pillars were found to be stable up to 700°C. The alumina pillared saponite exhibited peaks of 19 Å at room temperature and 16.9 Å at 700°C, indicating that pillar heights (or the slit widths) are 9.4 Å and 7.3 Å, respectively, after subtracting the thickness of the aluminosilicate layer (9.6 Å). The d-values of Al_2O_3 pillared montmorillonites are also very similar to those of saponite, except that the montmorillonite heated at 700°C gave a 16.0 Å spacing. The SiO_2-TiO_2 pillared clays exhibited much higher d(001)-values (Figure 2) compared with Al_2O_3 pillared samples. Typically, the d-values were 39 Å at room temperature but decreased to 32 Å at 500°C. These d-values are much higher than the values (17–19 Å) obtained by Occelli (1987) and Sterte and Shabtai (1987) for SiO_2-Al_2O_3 pillared clays. The d(002) and d(003) in these samples are not exactly multiple integrals of d(001), indicating that the layer expansion is apparently not uniform.

Adsorption properties

Adsorption-desorption isotherms. Water adsorption isotherms are presented in Figure 3. The alumina pillared saponite calcined at 400°C exhibited an enhanced adsorption at low relative pressure, whereas the adsorption at low relative pressure was depressed in the sample calcined at 700°C. The Al_2O_3 pillared montmorillonite calcined at 400°C showed a water adsorption isotherm that did not fit either the BET or the

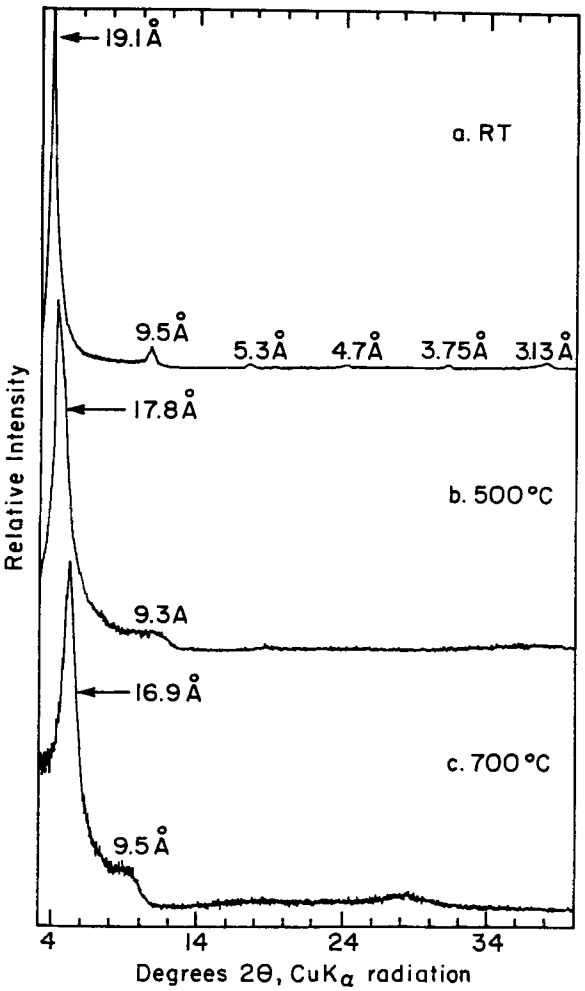

Figure 1. X-ray powder diffraction patterns of Al_2O_3 (APS) as a function of calcination temperature: a) room temperature (RT), b) 500°C, and c) 700°C.

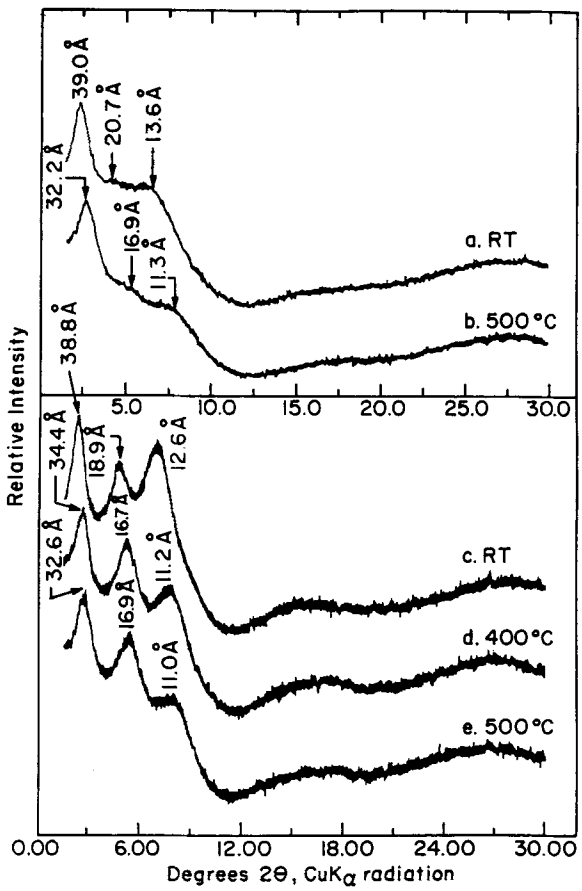

Figure 2. X-ray powder diffraction patterns of SiO_2-TiO_2 pillared smectites as a function of calcination temperature: a and b = saponite; c, d and e = montmorillonite; RT = room temperature.

Langmuir equation and that has been described earlier (Malla *et al.*, 1989) as an "unusual" isotherm shape (data not shown). The unusual shape has been attributed to development of hydrophobic sites after calcination (Yamanaka *et al.*, 1990; Malla *et al.*, 1989). Unlike water isotherms, N_2 adsorption in both Al_2O_3 pillared montmorillonite and saponite showed type I isotherms (Langmuir type) typical of microporous solids (Figure 4a). Both H_2O and N_2 isotherms exhibited hysteresis; and in the case of H_2O, the desorption branch did not meet the adsorption branch, even at a very low relative pressure, indicating an irreversible adsorption of water (possibly chemical reaction) on the surface of pillars and aluminosilicate layers (pore walls). The hysteresis loops in N_2 isotherms are of type H4 and indicate the presence of narrow slit-like micropores (Sing, 1985).

The SiO_2-TiO_2 pillared saponite exhibited a type IV isotherm (see Gregg and Sing, 1982) with H_2O (Figure 3), which indicates that the pores in these samples are large enough to show capillary condensation. The montmorillonite also exhibited a similar isotherm, except that the part of the isotherm near saturation was relatively flat compared with the saponite. As in the Al_2O_3 pillared clays, the desorption branch did not meet the adsorption branch even at low relative pressure, indicating a chemical reaction of H_2O molecules (hydroxylation) with pore walls. The N_2 adsorption isotherms of these clays are slightly different than those of Al_2O_3 pillared clays, that is, they exhibited isotherms transitional between type I and type IV (Figure 4a).

Surface area, pore volume and pore size. Nitrogen surface areas, pore volumes and pore sizes of the pillared clays are summarized in Table 2. Both alumina and silica-titania pillared clays exhibited large surface area and pore volume up to 700°C, although they decreased with increasing temperature. The pillared montmorillonites showed higher values compared to their saponite counterparts. The extent of decrease in surface area (Table 2) and micropore volume (data not shown) with increasing calcination temperature was, however, smaller for saponite than for montmorillonite. Addi-

https://doi.org/10.1346/CCMN.1993.0410408 Published online by Cambridge University Press

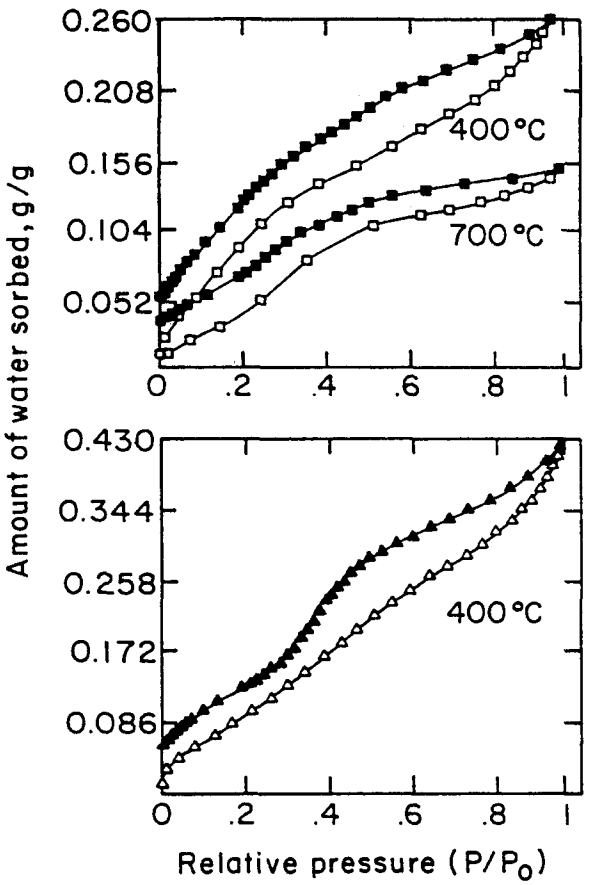

Figure 3. Water adsorption (open) and desorption (closed symbol) isotherms of the Al_2O_3 pillared saponite, (□, ■), APS at 400° and 700°C; as well as the SiO_2-TiO_2 pillared saponite (△, ▲), STPS at 400°C.

Table 2. Nitrogen adsorption properties of the pillared clays.

Sample[1]	$V_{t\text{-micro}}$ (cm^3/g) 400°C[2]	V_{total} (cm^3/g) 400°C[3]	S_{BET} (m^2/g)[4] 300°C	400°C	500°C	700°C	S_t (m^2/g) Micro 400°C	Meso 400°C
APM	0.157	0.217	427	414	386	280	382	32
APS	0.129	0.153	373	324	320	268	310	14
STPM	0.238	0.299	490	483	461	367	441	42
STPS	0.217	0.326	481	454	463	394	379	75

[1] See Table 1 for identification of samples.
[2] Slit width ≤20 Å.
[3] Total volume measured at p/po = 0.95.
[4] Linear fit at p/po = 0.02 − 0.1.
V = volume; micro = micropores; t = t-method; S = surface area; BET = BET method; meso = mesopores.

tionally, the SiO_2-TiO_2 pillared clays showed smaller decrease in surface area compared with alumina pillared clays when heated from 300° to 700°C, indicating higher stability of the former pillars.

Pore size distributions in both saponite and montmorillonite pillared with Al_2O_3 (Figure 4b) are very similar, with most of the pores having a diameter <20 Å with maxima at <10 Å. The SiO_2-TiO_2 pillared clays exhibited two maxima, one at <10 Å and another around 20 Å. The latter was broad and continued into the mesopore region before leveling off around 50 Å. The mesopores were minimized in Al_2O_3 pillared clays.

Magic-angle spinning (MAS) nuclear magnetic resonance (NMR) spectroscopy

^{27}Al spectrum of the original Na-saponite is given in Figure 5e. The chemical shift at 64.9 ppm can be attributed to Al^{IV} of the tetrahedral sheet. ^{27}Al spectra of Al_2O_3 pillared saponite are presented in Figures 5a–5d. The uncalcined sample (Figure 5a) exhibited the spectrum similar to Na-saponite (Figure 5e), except that a broad peak around −4 ppm due to Al^{VI} of the

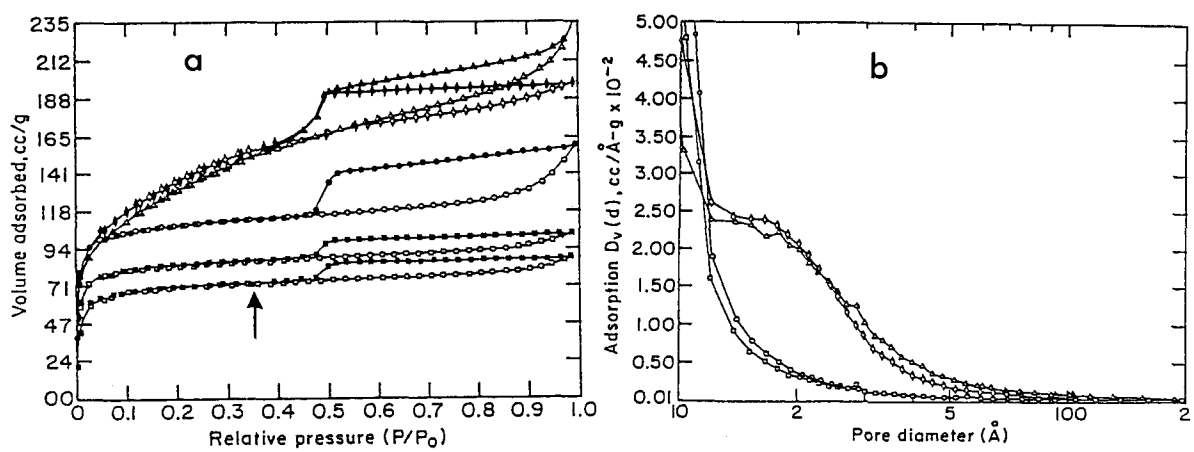

Figure 4. Nitrogen adsorption (open) and desorption (closed symbol) isotherms of the pillared smectites: In a) (○, ●), APM; (□, ■), APS; (◇, ◆) STPM; and (△, ▲) STPS. Abbreviations explained in Table 1. All samples were calcined at 400°C for 20 hr except the APS sample indicated by an arrow, which was calcined at 700°C for 4 hr. In b) pore size distribution of the pillared smectites calcined at 400°C calculated on the basis of adsorption isotherms shown in a).

https://doi.org/10.1346/CCMN.1993.0410408 Published online by Cambridge University Press

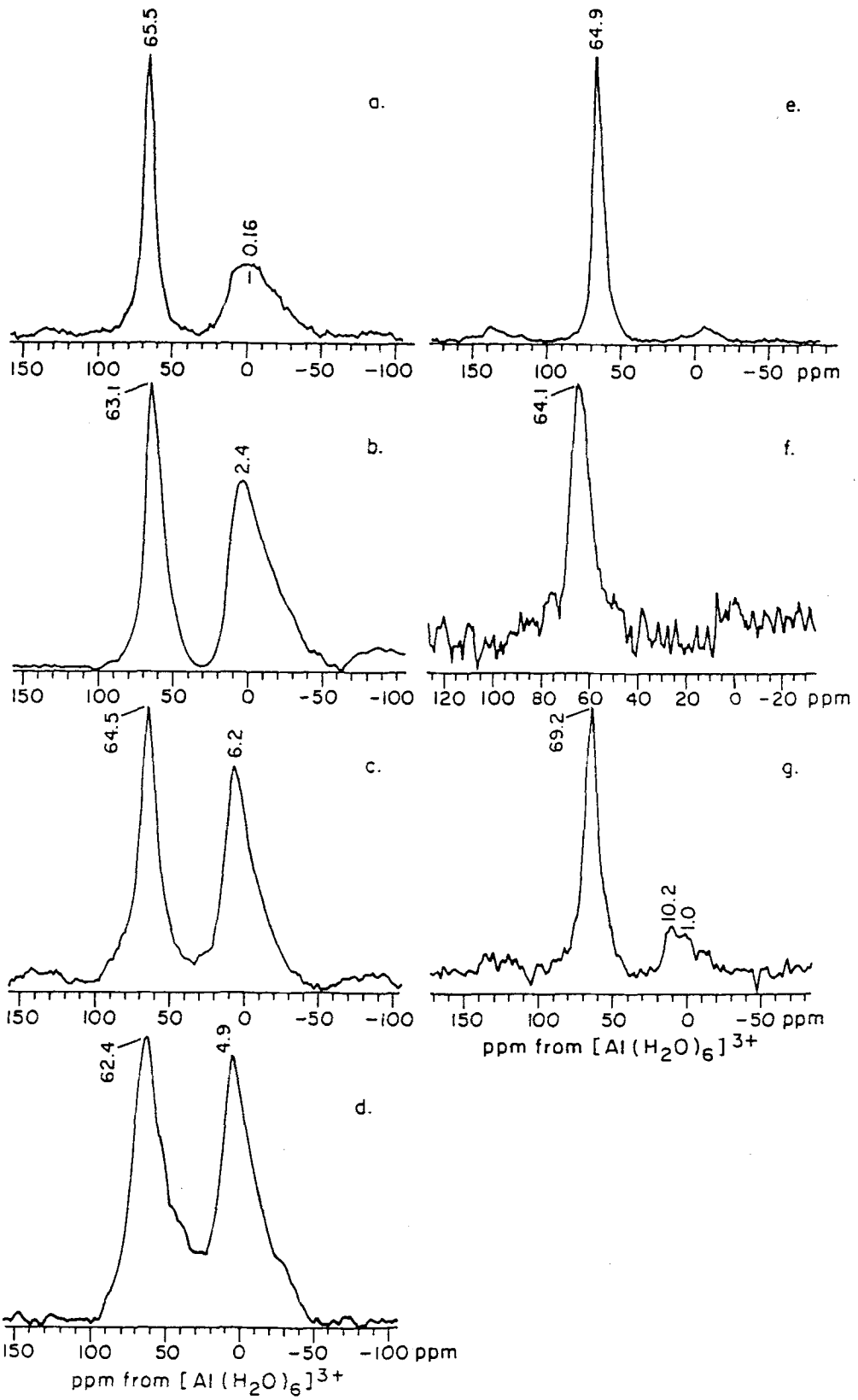

Figure 5. ^{27}Al MASNMR spectra of a) uncalcined APS, and calcined APS at b) 300°, c) 500° and d) 700°C, respectively, e) NaS, f) STPS (uncalcined), and g) STPS calcined at 500°C. Abbreviations explained in Table 1.

https://doi.org/10.1346/CCMN.1993.0410408 Published online by Cambridge University Press

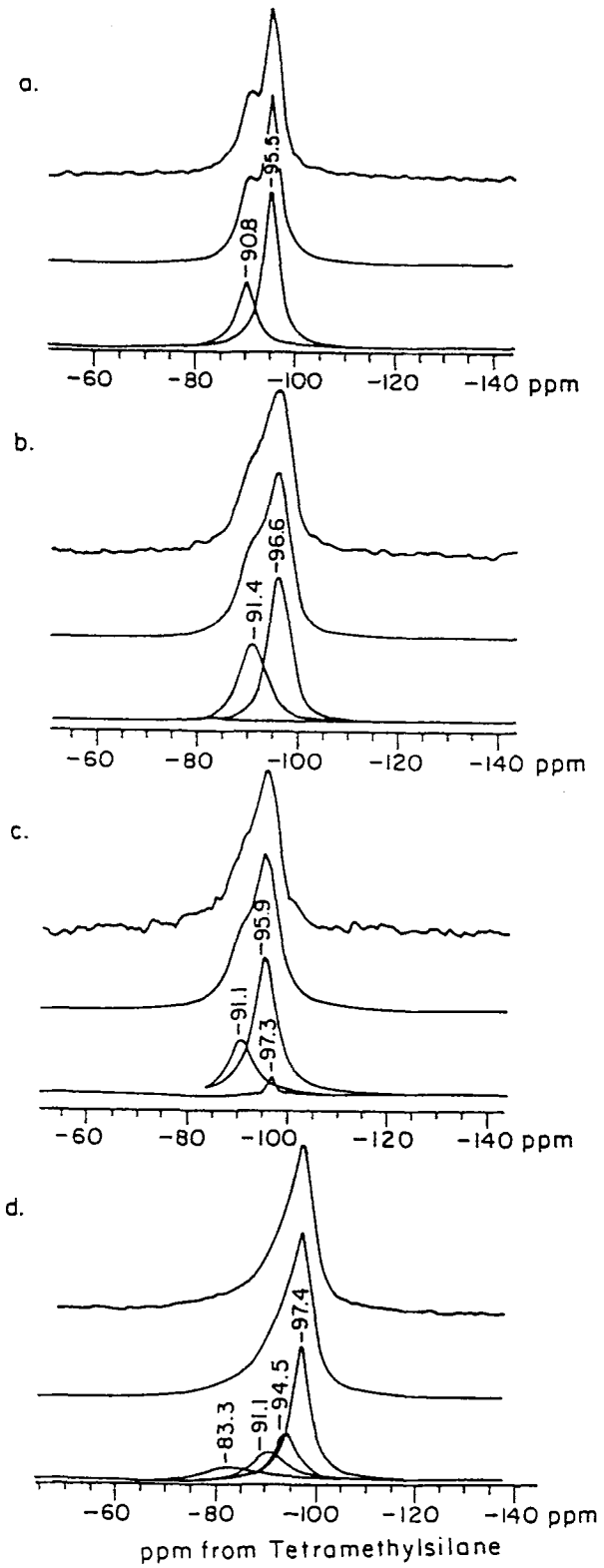

Figure 6. ^{29}Si MASNMR spectra of APS as a function of calcination temperature: a) uncalcined, b) 300°C, c) 500°C, and d) 700°C.

pillars was observed. The intensity of the peak due to Al^{VI} (2–6 ppm) increased after heating at 300°, 500°, and 700°C. The various thermal treatments also resulted in the narrowing of the peaks. At 700°C, a broad peak around 53 ppm (after deconvolution) appeared, indicating an evolution of distorted Al^{IV}. The original Na-montmorillonite showed a peak at 5.7 ppm, which can be assigned to octahedral Al^{VI}. The spectra of Al_2O_3 pillared montmorillonite before and after calcination at 500°C exhibited, in addition to Al^{VI} (7 and 3 ppm), small peaks at 73 and 67 ppm, respectively, indicating the presence of Al^{IV} from hydroxy-Al polymers (Al_{13}) in the interlayers (data not shown).

^{29}Si spectra of alumina pillared saponite before and after calcination and Na-saponite are given in Figures 6 and 7d. The $(Al/Si)^{IV}$ ratio, chemical shift, relative contribution of Si-nAl components, and peak widths are summarized in Table 4. The original Na-saponite exhibited two resonances at −90.6 and −95.6 ppm (Figure 7d), corresponding to Si(1Al) and Si(0Al) of the tetrahedral sheet. The Al_2O_3 pillared saponite (Figure 6a) exhibited a spectrum (−90.8 and −95.5 ppm) similar to that of Na-saponite. Calcination of the pillared sample at 300° (Figure 6b) and 500°C (Figure 6c) shifted the Si(0Al) and Si(1Al) resonances to slightly more negative values with a concomitant broadening of peaks, especially the Si (1Al) ones. At 700°C, a significant negative shift of Si(0Al) to −97.4 ppm (Figure 6d) occurred, with further broadening of Si(1Al) peak at −91.1 ppm. The Na- and Al_2O_3 pillared montmorillonite exhibited a single peak at −93.9 (Figure 7a) and −93.7 ppm (data not shown), respectively, which can be assigned to Si(0Al) of the tetrahedral sheet of the clay. Calcination of the Al_2O_3 pillared montmorillonite at 500°C gave a peak at −97 ppm. The more negative shift in ^{29}Si spectrum of calcined pillared samples has been attributed by Tennakoon *et al.* (1987) to neutralization of the layer charge by migrating protons liberated from the dehydration of Al_{13} pillars.

^{29}Si spectra of the SiO_2-TiO_2 pillared saponite are given in Figures 7e and 7f. The sample before calcination exhibited five resonances at −85.9, −90.5, −95.4, −101.1, and −110 ppm (Figure 7e). The first three peaks can be assigned to Si(2Al), Si(1Al), Si(0Al) of the clay tetrahedral sheet. The Si(2Al) was not observed in Na- or Al_2O_3 pillared saponite and is not included in the calculation of $(Al/Si)^{IV}$ ratio. The latter two correspond to OHSi(3Si) and Si(4Si) of the pillars. After calcination at 500°C, almost all the hydroxyl groups (silanol) were removed as indicated by the almost complete disappearance of the peak at −101.1 ppm that now appears at 101.3 ppm and the appearance of a broad peak at −107 ppm due to Si(4Si) (Figure 7f). Calcination also shifted the peak due to Si(0Al) to slightly more negative value (−96.3) and considerably broadened the peak due to Si(1Al). The SiO_2-TiO_2 pillared montmorillonite exhibited three peaks

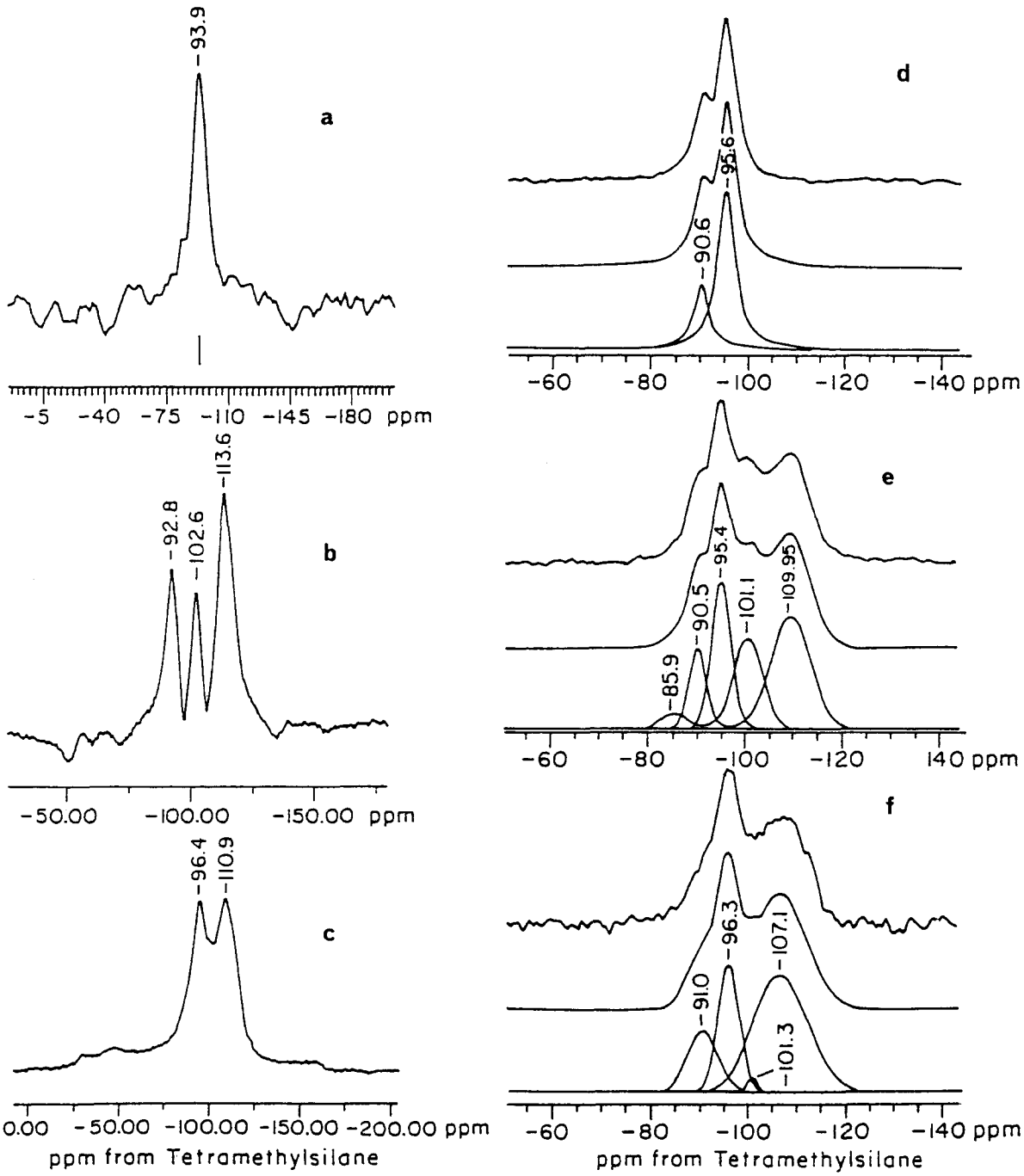

Figure 7. ^{29}Si MASNMR spectra of a) NaM, b) STPM (uncalcined), c) STPM (400°C), d) NaS, e) STPS (uncalcined), and f) STPS (500°C). Abbreviations explained in Table 1.

at −92.8 ppm, −102.6, and −113.6 ppm (Figure 7b), which can be assigned to the Si in the tetrahedral sheet, Si(0Al), and as in saponite, Si of the pillars, OHSi(3Si) and Si(4Si), respectively. The calcined SiO_2-TiO_2 pillared montmorillonite (Figure 7c) exhibited two peaks, one at −96.4 ppm attributable to the migration of protons towards the octahedral holes and another at −110.9 ppm attributable to the Si(4Si) of the pillars. The peak at −102.6 ppm disappeared after calcination due to the removal of silanol (OH) groups. Neither in saponite or montmorillonite was there any resonance that could be assigned to Si(nTi).

https://doi.org/10.1346/CCMN.1993.0410408 Published online by Cambridge University Press

Table 3. $(Al/Si)^{IV}$ ratio, ^{29}Si chemical shift ($-\delta$, ppm) and relative contribution (%) of Si-nAl components and full width at half maximum (fwhm, ppm) of saponite.

[1]Sample	$(Al/Si)^{IV}$		[4]Si-0 Al			[4]Si-1 Al		
	[2]Chem	[3]NMR	δ	%	fwhm	δ	%	fwhm
NaS	0.102	0.092	95.6	72.5	4.38	90.6	27.5	3.97
APSRT	0.102	0.111	95.5	66.8	3.63	90.8	33.2	4.33
APS300	0.102	0.137	96.6	58.1 (59)	5.36	91.4	40.4 (41)	6.88
APS500	0.102	0.097	95.9 97.3	67.4 3.1	5.43 1.86	91.1	29.4	5.97
APS700	0.102	0.066	94.5 97.4	20.9 (24.2) 48.2 (55.9)	5.36 4.45	91.1	17.1 (19.9)	7.29
STPSRT	0.102	0.109	95.4	24.9 (67.3)	4.81	90.5	12.11 (32.7)	4.33
STPS500	0.102	0.130	96.3	25.3 (61.1)	5.28	91.0	16.1 (38.9)	7.29

[1] From chemical analysis.
[2] See Table 1 for identification of samples; RT = room temperature; numbers following the samples are calcination temperature.
[3] Obtained from the following equation (Plee *et al.*, 1984): $(Al/Si)^{IV} = \Sigma_0^n$ nI(Si-n Al)/3.
[4] Values in parentheses are normalized to 100% for structural Si in Q^3 environment.

DISCUSSION

Pillaring species, basal spacings and adsorption properties

Generally, it has been accepted that the pillaring species in hydroxy-Al solution is similar to the cationic polymer, $[Al_{13}O_4(OH)_{24}(H_2O)_{12}]^{7+}$ (Vaughan, 1988; Pinnavaia *et al.*, 1984). In the case of SiO_2-TiO_2 pillaring solution, positively charged sol particles are formed during hydrolysis and condensation of monomeric alkoxides in acid medium and are exchanged in the clay. The positively charged sol particles can be achieved two ways: 1) incorporating TiO_2 (isoelectric point of TiO_2 is around pH 6) in the network of SiO_2 (isoelectric point of SiO_2 is around pH 2); and/or 2) coating the SiO_2 particles with positively charged TiO_2 particles. In the SiO_2-TiO_2 (binary) system, the rates of hydrolysis of Si and Ti alkoxides are different and, therefore, there is little or no incorporation of Ti in the SiO_2 network unless the hydrolysis of Ti-isopropoxide is carried out in a controlled manner using a chelating agent (LaCourse and Kim, 1986). Since the rates of hydrolysis of the alkoxides were not controlled in this study, little or no incorporation of Ti in the SiO_2 network was expected. In fact, we did not see any peak that could be assigned to Si(nTi) in ^{29}Si NMR spectra. Thus, the SiO_2 particles that were coated with

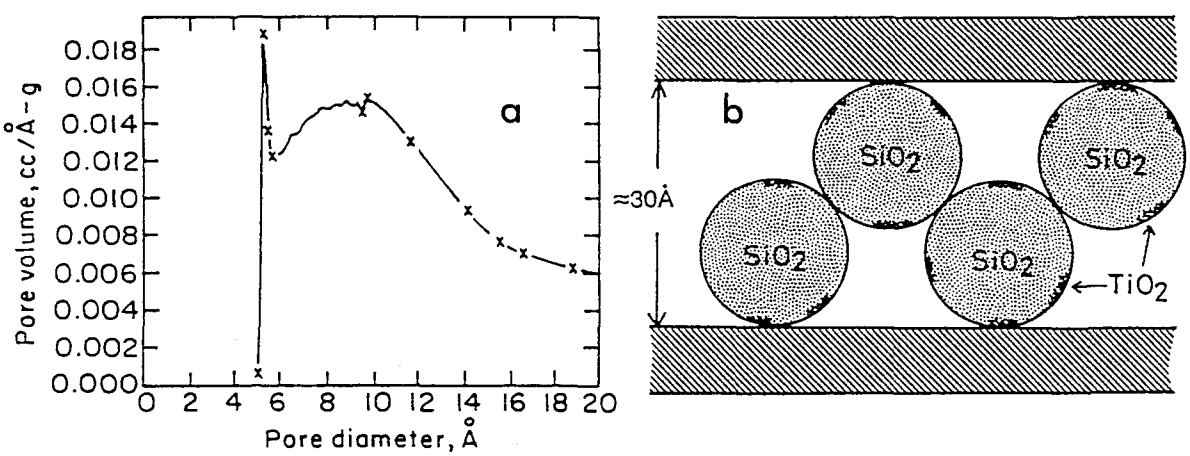

Figure 8. a) Micropore size distribution (Horvath and Kawazoe method) of STPS (400°C), and b) structural model showing arrangement of SiO_2-TiO_2 particles in STPS and STPM (after Yamanaka *et al.*, 1988).

https://doi.org/10.1346/CCMN.1993.0410408 Published online by Cambridge University Press

positively charged TiO_2 particles must have been intercalated as suggested by Yamanaka *et al.* (1988).

In the Al_2O_3 pillared clays, the XRD slit widths (7–9 Å) are approximately equal to the micropores (<10 Å) estimated from the gas adsorption isotherms (Figure 4; Michot and Pinnavaia, 1992). This is, however, not the case in SiO_2-TiO_2 pillared samples. For example, XRD showed the slit widths to be about 24 Å after calcination at 400°C, whereas the pore size distribution curves using the Kelvin equation indicated that most of the pore diameters are to be <20 Å, or even <10 Å. Since the Kelvin equation is not quite valid for pore diameters <20 Å, Ar adsorption over the relative pressure range $10^{-6} < P/Po < 0.99$ was performed and micropore size distribution was determined using the Horvath-Kawazoe model (Horvath and Kawazoe, 1983). In fact most of the pores were found to be <20 Å with a broad distribution (Figure 8a). Despite a high basal spacing, the preponderance of micropores in the SiO_2-TiO_2 pillared samples can be visualized from the multilayer intercalation of SiO_2-TiO_2 sol particles and the formation of micropores in interstices between intercalated particles and silicate layers (Figure 8b). The SiO_2-TiO_2 pillared clays also consisted of a significant amount of mesopores (Figure 4b) whose pore size distribution leveled off around 50 Å. The mesopores probably formed either at the frayed edges or in between the crystallites. The presence of both micropores and mesopores with broad distributions may have contributed to the transitional type of isotherm shape (Figure 4) of these pillared clays. A similar isotherm shape was observed by Gregg and Sing (1982) for a sample having two types of micropores: small (<7 Å) and large (<18 Å).

Cross-linking

Both ^{27}Al and ^{29}Si MAS-NMR results in Al_2O_3- and SiO_2-TiO_2 pillared montmorillonites indicated that no direct cross-linking between the pillars and the structure occurs at the calcination temperature studied. These results are in agreement with the previous ^{27}Al and ^{29}Si MASNMR studies of alumina pillared clays having octahedral location of charge (montmorillonites and hectorites) (Tennakoon *et al.*, 1986; Plee *et al.*, 1985).

Unlike montmorillonite, pillared saponite exhibited many differences before and after calcination in the ^{27}Al and ^{29}Si MAS-NMR spectra, indicating considerable structural modifications. The striking features of the Al_2O_3 pillared saponite are: 1) increased intensity of the peak due to Al^{VI} (2–6 ppm) in relation to Al^{IV} as the temperature of calcination (300° to 700°C) increased; 2) more negative shift and broadening of Si(0Al) and Si(1Al) resonances in ^{29}Si as a function of increased calcination temperature; 3) lower than the stoichiometric amount of Al (63% of the total, as in Table 1) due to Al^{VI} in ^{27}Al spectrum (Figure 5a), indicating that the electric field gradient effects in saponite interlayers are large compared to other clays and that part of Al^{VI} of pillars escaped detection; and 4) no separate resonances for Al^{IV} of pillars and tetrahedral sheet because of the overlapping of both resonances at 63–65 ppm. The first two features are discussed in detail below.

The large increase in intensity of Al^{VI} resonance relative to Al^{IV} with increased calcination temperature can be attributed, in addition to the possible effect of reduced quadrupole interaction after thermal treatment, to a removal of Al from the tetrahedral sheets of saponite. In fact, such de-alumination has been deliberately carried out in NH_4-exchanged zeolite Y at >400°C in the presence of steam in order to make the zeolite ultrastable without significantly affecting its crystallinity (McDaniel and Maher, 1976). In alumina pillared clays, protons are released during the dehydroxylation of Al_{13} pillars,

$$[Al_{13}O_4(OH)_{24}(H_2O)_{12}]^{7+} \rightarrow 6.5\,Al_2O_3 + 8.5\,H_2O + 7H^+$$

and these protons are apparently responsible for hydrolytic splitting of SiOAl bonds followed by the removal of part of the tetrahedral Al in saponite. The vacant sites created after dealumination can be thought to have been occupied by Si that has migrated from the part of the collapsed clay structure to form Si-O-Si bonds at temperatures ≥500°C. This thesis is also supported by the fact that the water adsorption isotherm of saponite heated at 700°C was depressed at low relative pressure and did not fit either the BET or the Langmuir equation. This can be attributed to the development of hydrophobic sites resulted from the loss of protons and the formation of Si-O-Si bonds. No apparent change in pore size was observed. The samples heated at ≤400°C, however, did not exhibit the unusual shape of isotherm due to presence of hydrophilic sites, such as H^+ and/or OH groups. The sample heated at 500°C exhibited an isotherm shape intermediate of samples heated at 400° and 700°C, indicating that the hydrolytic splitting of the SiOAl bonds was completed somewhere in between 500° and 700°C. The de-alumination process also renders zeolites hydrophobic due to the formation of Si-O-Si bonds (Chen, 1976). Although a similar mechanism of cleavage of SiOAl bonds by proton attack in pillared beidellite has been proposed by Plee *et al.* (1985) and Schutz *et al.* (1987), they did not observe the increase of Al^{VI} in NMR spectra as has been observed in this study for saponite. As in Al_2O_3 pillared saponite, ^{27}Al spectrum of SiO_2-TiO_2 pillared saponite heated at 500°C, in addition to Al^{IV}, also exhibited a small but broad peak around 0 ppm (Figure 5g), indicating the presence of Al^{VI}. Such peak was not observed in the uncalcined sample (Figure 5f). Since the only source

of Al in this sample is tetrahedral sheet, the peak around 0 ppm in calcined sample must be the consequence of some degree of de-alumination of the tetrahedral sheet.

The modification of tetrahedral sheets started as low as 300°C, as indicated by peak broadening and a slightly negative shift of Si(0Al) peak. The $(Al/Si)^{IV}$ (NMR) of alumina pillared samples decreased with increasing calcination temperature (Table 3) (except for sample calcined at 300°C, APS300), which supports the de-alumination process observed by ^{27}Al. The increased $(Al/Si)^{IV}$ (NMR) in APS300 is due to the broadening of a peak centered at −91.4 ppm. The broad peaks at −96.6 can be thought of as a composite of two peaks at −95.5 (sample not calcined, APSRT) and −97.4 (sample calcined at 700°C, APS700). Similarly, the peak at 91.4 ppm can be thought of as being composed of peaks at −90.8 and −94.5 ppm. The peak broadening can be attributed to at least one or both of the following reactions: 1) initiation of hydrolytic splitting of Si-O-Al linkages which modifies the Si environment and 2) initiation of inversion of SiO_4 tetrahedra and its bonding with Al^{VI} of the pillar which place the Si in the $Q^4(1Al)$ environment as suggested by Pinnavaia *et al.* (1985b) for fluorohectorite. The effect of the former reaction is to broaden the Si(1Al) peak and that of the latter is to broaden the peak centered at −96.6 ppm due to overlapping of two Si(0Al) peaks, that is, $Q^3(0Al)$ (−95.5 ppm) and $Q^4(Si)(1Al)$ (−97.4 ppm). The modification of tetrahedral sheet was much more evident in sample heated at 700°C. Unlike the sample heated at 300° and 500°C, the sample heated at 700°C has such a large amount of $Q^4(1Al)$ that a relatively narrow and intense peak at −97.4 ppm for $Q^4(1Al)$ is evident. Assuming that only $Q^3(Si)(0Al)$ reacted with the pillar, Table 3 (Figure 6d) indicates that 84% of $Q^3(Si)(0Al)$ or 56% of the total SiO_4 tetrahedra have reacted and 39% of the total $Q^3(Si)(nAl)$ or 13% of $Q^3(Si)(1Al)$ was rendered without Al as next neighbor. Although NMR spectra of SiO_2-TiO_2 pillared saponite at temperatures >500°C were not obtained, the results indicate that reactions similar to those observed in alumina pillared saponite may also occur in this system. The higher stability of pillared saponites (both Al_2O_3 and SiO_2-TiO_2) compared with montmorillonite at 700°C (as judged from the extent of decrease in surface area) may have been achieved as a result of the cross-linking and the formation of Si-O-Si bonds. In addition to a higher thermal stability, the structural modification of pillared saponite is expected to offer unique properties useful in adsorption and catalysis.

ACKNOWLEDGMENTS

This study was performed at Materials Research Laboratory, The Pennsylvania State University, and supported by the Gas Research Institute under contract #5087-260-1473.

REFERENCES

Barrer, M. and MacLoed, D. M. (1955) Activation of montmorillonite by ion exchange and sorption complexes of tetra-alkylammonium montmorillonites: *Trans. Faraday Soc.* **51,** 1290–1300.

Barrett, E. P., Joyner, L. G., and Halenda, P. P. (1951) The determination of pore volume and area distributions in porous substances. I. Computations from nitrogen isotherms: *J. Am. Chem. Soc.* **73,** 373–380.

Bellaoui, A., Plee, D., and Meriaudeau, P. (1990) Gallium containing pillared interlayer clays. Preparation, characterization and catalytic properties: *Appl. Catal.* **63,** L7–L10.

Brindley, G. W. and Sempels, R. E. (1977) Preparation and properties of some hydroxy-aluminum beidellites: *Clays & Clay Minerals* **12,** 229–236.

Cariati, F., Erre, L., Micera, G., Piu, P., and Gessa, C. (1983) Effect of layer charge on the near-infrared spectra of water molecules in smectites and vermiculites: *Clays & Clay Minerals* **31,** 447–449.

Chen, Y. (1976) Hydrophobic properties of zeolites: *J. Phys. Chem.* **80,** 60–64.

Gonzalez, F., Pesquera, C., Blanco, C., Benito, I., and Mendioroz, S. (1992) Synthesis and characterization of Al-Ga pillared clays with high thermal and hydrothermal stability: *Inorg. Chem.* **31,** 727–731.

Gregg, S. J. and Sing, K. S. W. (1982) *Adsorption, Surface Area and Porosity:* 2nd ed., Academic Press, New York, 303 pp.

Harward, M. E. and Brindley, G. W. (1965) Swelling properties of synthetic smectites in relation to lattice substitutions: *Clays & Clay Minerals* **3,** 209–222.

Harward, M. E., Carstea, D. D., and Sayegh, A. H. (1969) Properties of vermiculites and smectites: Expansion and collapse: *Clays & Clay Minerals* **16,** 437–447.

Horvath, G. and Kawazoe, K. (1983) Methods for the calculation of effective pore size distribution in molecular sieve carbon: *J. Chem. Eng. Jpn.* **16,** 470–475.

Ingamells, C. O. (1970) Lithium metaborate flux in silicate analysis: *Anal. Chemica Acta* **52,** 323–334.

Jackson, M. L. (1969) *Soil Chemical Analysis—Advanced Course:* 2nd ed., published by author, Department Soil Science, University of Wisconsin, Madison, Wisconsin, 895 pp.

LaCourse, W. C. and Kim, S. (1986) Use of mixed titanium alkoxides for sol-gel processing: in *Science of Ceramic Chemical Processing,* L. L. Hench and D. R. Ulrich, eds., John Wiley & Sons, New York, 304–310.

McDaniel, C. V. and Maher, P. K. (1976) Zeolite stability and ultrastable zeolites: in *Zeolite Chemistry and Catalysis, 1976, ACS Monograph* **171,** J. A. Rabo, ed., American Chemical Society, Washington D.C., 285–331.

Malla, P. B. and Douglas, L. A. (1987) Layer charge properties of smectites and vermiculites: tetrahedral *vs.* octahedral: *Soil Sci. Soc. Am. J.* **51,** 1362–1366.

Malla, P. B., Yamanaka, S., and Komarneni, S. (1989) Unusual water vapor adsorption behavior of montmorillonite pillared with ceramic oxides: *Solid State Ionics* **32/33,** 354–362.

Malla, P. B. and Komarneni, S. (1990a) Synthesis of highly microporous and hydrophilic alumina-pillared montmorillonite: Water-sorption study: *Clays & Clay Minerals* **38,** 363–372.

Malla, P. B. and Komarneni, S. (1990b) Effect of crystal chemistry on pore structure and hydrophilicity of alumina-pillared smectites: Water sorption study: *Sci. Geol., Mem.* **86,** 59–68.

Medlin, J. H., Suhr, N. H., and Bodkin, J. B. (1969) Atomic absorption analysis of silicate employing $LiBO_2$ fusion: *Atomic Abs. News Lett.* **8,** 25–29.

Michot, L. J. and Pinnavaia, T. J. (1992) Improved synthesis of alumina-pillared montmorillonite by surfactant modification: *Chem. Mater.* **4,** 1433–1437.

Mortland, M. M. and Raman, K. V. (1968) Surface acidity of smectites in relation to hydration, exchangeable cation, and structure: *Clays & Clay Minerals* **16,** 393–398.

Occelli, M. L. (1987) Surface and catalytic properties of some pillared clays: in *Proc. Int. Clay Conf., Denver, 1985,* L. G. Schultz, H. van Olphen, and F. A. Mumpton, eds., The Clay Minerals Society, Bloomington, Indiana, 319–323.

Pinnavaia, T. J., Tzou, M., Landau, S. D., and Raythatha, H. (1984) On the pillaring and delamination of smectite clay catalysts by polyoxo cations of aluminum: *J. Mol. Catal.* **27,** 195–212.

Pinnavaia, T. J., Tzou, M., and Landau, S. D. (1985a) New chromia pillared clay catalysts: *J. Amer. Chem. Soc.* **107,** 4783–4785.

Pinnavaia, T. J., Landau, S. D., Tzou, M., and Johnson, I. D. (1985b) Layer cross-linking in pillared clays: *J. Amer. Chem. Soc.* **107,** 7222–7224.

Plee, D., Borg, F., Gatineau, L., and Fripiat, J. J. (1985) High resolution solid state ^{27}Al and ^{29}Si nuclear magnetic resonance study of pillared clays: *J. Amer. Chem. Soc.* **107,** 2362–2369.

Plee, D., Borg, F., Gatineau, L., and Fripiat, J. J. (1987) Pillaring processes of smectites with and without tetrahedral substitution: *Clays & Clay Minerals* **35,** 81–88.

Robert, M. (1973) The experimental transformation of mica toward smectite. Relative importance of total charge and tetrahedral substitution: *Clays & Clay Minerals* **21,** 167–174.

Schutz, A., Stone, W. E. E., Poncelet, G., and Fripiat, J. J. (1987) Preparation and characterization of bidimensional zeolitic and hydroxy-aluminum solutions: *Clays & Clay Minerals* **35,** 251–261.

Sing, K. S. W. (1985) Reporting physisorption data for gas/solid systems: *Pure Appl. Chem.* **57,** 603–619.

Sterte, J. (1986) Synthesis and properties of titanium oxide cross-linked montmorillonite: *Clays & Clay Minerals* **35,** 658–664.

Sterte, J. and Shabtai, J. (1987) Cross-linked smectites. V. Synthesis and properties of hydroxy-silicoaluminum montmorillonites and fluorohectorites: *Clays & Clay Minerals* **35,** 429–439.

Tennakoon, D. T. B., Jones, W., and Thomas, J. M. (1986) Structural aspects of metal-oxide-pillared sheet silicates: *J. Chem. Soc., Farad. Trans. I* **82,** 3081–3095.

Tennakoon, D. T. B., Jones, W., Thomas, J. M., Ballantine, J. H., and Purnell, J. H. (1987) Characterization of clay and pillared clay catalysts: *Solid State Ionics* **24,** 205–212.

Van Olphen, H. (1966) Collapse of potassium montmorillonite clays upon heating—"Potassium fixation": *Clays & Clay Minerals* **14,** 393–405.

Vaughan, D. E. W. (1988) Pillared clays—A historical perspective: *Catal. Today* **2,** 187–198.

Weir, J. I. and White, J. L. (1951) Potassium fixation in clay minerals as related to crystal structure: *Soil Sci.* **71,** 1–14.

Yamanaka, S. and Brindley, G. W. (1979) High surface area solids obtained by reaction in montmorillonite with zirconyl chloride: *Clays & Clay Minerals* **27,** 119–124.

Yamanaka, S., Nishihara, T., and Hattori, M. (1987) Preparation and properties of titania pillared clays: *Materials Chemistry Physics* **17,** 87–101.

Yamanaka, S., Nishihara, T., and Hattori, M. (1988) Adsorption and acidic properties of clays pillared with oxide sols: in *Microstructure and Properties of Catalysts, Proc. Materials Research Society, Boston, Massachusetts, 1987,* **111,** M. M. J. Treacy, J. M. Thomas, and J. M. White, eds., Materials Research Society, Pittsburgh, Pennsylvania, 283–288.

Yamanaka, S., Malla, P. B., and Komarneni, S. (1990) Water adsorption properties of alumina-pillared clays: *J. Colloid Interface Sci.* **134,** 51–58.

Yamanaka, S. and Komarneni, S. (1991) Apparatus for measuring liquid vapor adsorption and desorption characteristics of a sample: U.S. Patent **5,058,442,** October 22, 1991.

(Received 19 June 1992; accepted 7 June 1993; Ms. 2236)